

Understanding Power MOSFET Saturation Operation Capability

AND90187/D

A power MOSFET can be operated in four different operating modes: as a switch, called ohmic or linear¹ operating mode, in diode conduction mode, in avalanche mode, and in saturation mode. MOSFET saturation mode is illustrated in figure 1 below, which shows a power MOSFET I_d vs V_{ds} and V_{gs} curves (this plot displays first quadrant operation only, so diode condition is not shown and with V_{ds} truncated so avalanche operation is not shown). MOSFET saturation mode is defined as operation with high V_{ds} , specifically where $V_{ds} > (V_{gs} - V_{th})$. In saturation operation, device power is given by $V_{ds} \times I_d$, not by $I_d^2 \times R_{ds(on)}$.

Power MOSFET saturation operation is important to understand for several reasons. First, saturation operation occurs in nearly every type of application utilizing MOSFETs. There are many applications where the application function depends on MOSFET saturation operation. These include linear voltage regulation, linear DC motor control, class A and AB audio amplification, current in-rush control, (e.g., hot swap), active clamp control for unclamped inductive loads, and airbag “safing” FET operation. And what may not be realized is that a power MOSFET operates in saturation during each switching transition, as the device V_{ds} transits thru the Miller plateau region. Second, at high current and high V_{ds} operation, device power is much higher than in linear switch-mode operation and therefore thermal management may be an important design consideration. Third, a MOSFET operating in saturation may be susceptible to thermal runaway, leading to device failure at a supposedly safe device power level. It is this third point which is the focus of this application note: to describe MOSFET thermal instability in saturation operation and to understand how to utilize power MOSFET data sheet safe operating (FBSOA) plot data.

Thermal stability can first be described in general terms considering a system containing some general device that dissipates power and some methodology for the system to sink heat generated by the device power dissipation. Consider the three diagrams in figure 2². The green curve in each plot is the same; this represents the system capability to sink heat: the slope of the line is given by the reciprocal of the system thermal resistance, or dQ / dT_j , where Q is used to represent device power and T_j represent device junction temperature. The intersection of the system line and the x-axis represents the initial device junction temperature (at

$Q = 0$), labeled as T_x . The device line in each curve shows the device power dissipation as a function of T_j . In the first plot, at left, the device line slope is less than the system line. In this case the system can absorb more heat than the device can generate, and a stable thermal operating point is possible. In the middle plot, the device line slope is greater than the system line. In this case, device power increases faster than the system can pull heat from the device and thermal runaway results. The right plot shows a non-linear device power function, which is more likely in real world applications, where it is possible both for thermal stable operation and thermal runaway operating points.

Thermal runaway for a MOSFET almost always results in device destruction. Figure 3 shows the typical result, a burn spot on the die commonly labeled as “EOS” (electrical overstress) failure. What happens in a thermal runaway event is that the hottest spot on the die surface, determined by the physical boundary conditions of the die and package designs, such as source clip placement, reaches intrinsic temperature. At this point the hot spot area becomes a conductor and the resultant high current density increases the temperature in the area to levels that device structures begin to melt together. This results in a vertical “filament” thru the die and electrically measures as a drain to source to gate low ohmic short. Why this happens is illustrated in figure 4. This shows the transconductance curve of a power MOSFET, which is the plot of $I_d(sat)$ vs V_{gs} , for a device operating in saturation at some specified V_{ds} value. Typically, curves are shown for three different junction temperatures, however some plots may include data for two junction temperatures.

One obvious attribute of this plot is that the curves representing different junction temperature values intersect at a single point. This means that $I_d(sat)$ is independent of junction temperature at some V_{gs} value, referred to as $V_{gs}(ZTC)$, where ZTC stands for “zero temperature coefficient). The reason this happens is that the MOSFET saturation current function (equation 1) includes two main temperature dependent variables: threshold voltage, V_{th} , and mobility, μ_0 . The general forms of mobility and threshold as functions of junction temperature, T_j , are listed as equations 2 and 3. For a MOSFET in saturation at higher V_{gs} , the mobility term dominates and at lower V_{gs} , the delta V_{gs} to V_{th} term dominates, creating the crossing transconductance functions with respect to temperature.

1. In practice, engineers often refer to saturation operation as “linear mode”; this because they consider the MOSFET operation in an application, such as linear regulator function, not the operating mode of the MOSFET device itself.
2. Refer to [onsemi](#) application note [AND8223/D](#) “Predicting Thermal Runaway” for complete discussion on this topic.

Another way to visualize this is shown in figure 5, which plots $I_d(\text{sat})$ as function of T_j for increasing V_{gs} values. In this example, $I_d(\text{sat})$ is constant with respect to T_j at $V_{gs}(\text{ZTC}) = \sim 5.2$ V. At V_{gs} values above this, $I_d(\text{sat})$ has a negative temperature coefficient with respect to T_j and for V_{gs} values lower the $V_{gs}(\text{ZTC})$ the $I_d(\text{sat})$ temperature coefficient is positive.

$$I_{dsat} \cong \frac{\mu_o \cdot C_{ox} \cdot W}{2 \cdot L} \cdot (V_{gs} - V_{th})^2 \quad (\text{eq. 1})$$

$$\mu(T) = \mu_o \cdot \left(\frac{T}{T_o}\right) - \gamma \quad (\text{eq. 2})$$

$$V_{th}(T) = V_{th_o} \cdot (1 - m \cdot (T - T_o)) \quad (\text{eq. 3})$$

It is when the $I_d(\text{sat})$ temperature coefficient is positive that thermal runaway is possible. Referring to the general discussion about thermal instability, if the device power is increasing as T_j increases at a rate greater than the system can sink the added heat, the device junction temperature will runaway and device failure results. This can only happen if the device is operating in saturation and operating at V_{gs} values below $V_{gs}(\text{ZTC})$, where the I_{dsat} temperature coefficient is positive. Simply said thermal runaway can occur when the device generates more power (P_{gen}) than the system can dissipate (P_{dis}). Equations 4 and 5 define P_{gen} and P_{dis} respectively and if we define thermal instability where $P_{gen} > P_{dis}$, then this function can be described by equation 6. From this equation it is clear thermal instability can occur only if the $I_d(\text{sat})$ temperature coefficient is positive.

$$P_{gen} = I_{dsat}(T) \cdot V_{ds} \quad (\text{eq. 4})$$

$$P_{dis} = dT / r(t) \quad (\text{eq. 5})$$

$$P_{gen} > P_{dis} \rightarrow I_{dsat}(T) \cdot V_{ds} > dT / r(t) \rightarrow \frac{I_{dsat}(T)}{dT} \cdot V_{ds} > 1 / r(t) \quad (\text{eq. 6})$$

Thermal instability can be visualized if we measure dT_j as a function of increasing power for a power MOSFET device operated in saturation. If a device is operating with a stable thermal operating point, then dT_j as a function of power should measure as a linear function. That is, we expect $dT_j = P_d / r(t)$. One method to make such a plot is to measure a device in saturation at a constant V_{ds} value and increment current, measuring dT_j response for some given pulse duration. We then plot dT_j as a function of I_d and expect a linear response if the device is not in thermal instability region. Figure 6 shows two examples of such plots each at different V_{ds} values and different pulse durations. In both plots we can observe initially (at lower I_d values) the linear thermal response expected. However, at some I_d (i.e., power) value, the dT_j response increases much more than expected, indicating the onset of thermal instability operation. In the right-hand plot, the device reached failure; one can observe the rapid dT_j/I_d for the measurements just prior to failure — this is thermal runaway.

The physical mechanism of thermal runaway can be observed by taking device to failure and then perform physical analysis of the failed units. As discussed earlier, the power MOSFET, if subject to thermal runaway failure, will fail at a position that correlates to the hottest spot on the die. This spot (note that some refer to thermal runaway as “hot-spotting failure”) is determined by the physical construction of the device. Refer to figure 7 which shows two different constructions using the same package (SO8FL) and same silicon die. The only difference between the two is the source clip design. The hottest spot on the die correlates to the area near that of highest front (surface) metal current density. In the left design, there is a larger section of die active area not covered by the source clip compared to the right design. These devices were taken to failure in saturation operation (thermal runaway). The failure location on the die shifts to the left for the smaller clip design, correlating to an area near highest front metal current density. This result shows that thermal instability is not only function of die technology and electrical attributes, but also the thermomechanical design of the total device.

To measure saturation capability requires a circuit like that blocked out in figure 8. The circuit needs to drive the MOSFET such that a constant drain current, I_d , and constant drain to source voltage, V_{ds} , is achieved for the full pulse width. A standard current sink circuit is utilized to control both I_d and pulse duration. A separate bias circuit forces constant V_{ds} whilst affording gate to source voltage, V_{gs} , to vary during the pulse duration as needed to maintain the constant I_d and V_{ds} target values. Such circuitry is available commercially, although maximum allowed power and minimum pulse duration can be limiting to a full characterization for the device. In these cases, manual bench top set-ups are employed. Standard characterization methodology is to set a V_{ds} value, and increment I_d until failure, and repeat for multiple V_{ds} values and pulse durations. The collection of $I_d(\text{fail})$ values for a given pulse duration can be fitted to a function. This technique is illustrated in the right-hand side of figure 8. The $I_d(\text{fail})$ data typically fits to a power function of the form: $I_d = \text{constant} \times V_{ds}^{-\alpha}$, where the exponent magnitude, α , is >1 . This function clearly indicates that device power capability decreases significantly as V_{ds} increases, another indication of the thermal instability effect (refer to equation 6).

Although pulsed saturation capability can ideally be measured for any pulse duration, including up to steady state operation, there are practical limitation to consider. First, as apparent from equation 6, the application thermal system affects saturation operation capability. For typical power MOSFET packages and associated application thermal management (PCB and heat sink design), the system external thermal boundaries only appreciably affect heat flow for pulse duration greater than approximately 10 ms. Therefore, especially on more recent datasheets, pulsed saturation capability is published for pulse durations ≤ 10 ms. Note that if longer pulse durations are specified, the

associated external thermal boundary conditions for the device in the system environment should be specified. On the short pulse duration side, it is difficult to measure higher current capability at pulse durations less than ~300 ms on commercial equipment, and perhaps <~100 ms on manual setups. The issue is the current waveform becomes trapezoidal in shape at shorter pulse duration and high current, due to stray inductance in the test circuit and slew rate control to avoid significant current overshoot.

Figure 9 displays measured pulsed saturation capability (pulse duration = 1 ms in this example) comparing planar technology to second, third, and fourth generation trench technologies. The y-axis is current density (normalized to die active area) so that multiple technology and die area data can be included in the same plot. Also shown on the plot is a normalized constant power curve, which is the expected safe power capability of the device for a 1 ms duration power pulse, assuming a given dT_j (in this example $dT_j = 150^\circ\text{C}$). There are two important observations to consider on this plot. One, is that the power function of planar is less steep compared to trench technology data (lower exponent value). Because of this, the other important consideration is that the planar $I_d(\text{fail})$ data remains greater than the calculated safe thermal capability, whereas the trench technology $I_d(\text{fail})$ data measure less than the safe calculated thermal capability at higher V_{ds} voltages. This is an important observation when discussing FBSOA plot formation later in this paper.

Power MOSFET pulsed saturation capability is included in the data sheet FBSOA (forward bias safe operating area) plot (refer to figure 10). The FBSOA plot, included on MOSFET data sheets since production inception in late 70s to early 80s, is based on the power bipolar transistor active region SOA data sheet plots. These plots were designed to show device wire bond collector current capability, thermally limited power capability, and power limitation due to secondary breakdown. The power MOSFET FBSOA plot is designed for similar information, including pulsed current limit (in ohmic mode), absolute maximum V_{ds} operation, thermal limit in saturation operation, and saturation operation limited by thermal instability. The power MOSFET FBSOA plot also includes limitation due to $R_{ds(\text{on})}$, which is simply the slope on the curve that represents the maximum $R_{ds(\text{on})}$ value at maximum junction temperature. Note that the safe operating area for ohmic operation (i.e., limited by $R_{ds(\text{on})}$) is *above* the $R_{ds(\text{on})}$ maximum line on the plot).

If we focus on the pulsed saturation portion of the FBSOA plot curves, we find that the plot indicates limitation due to thermal capability and limitation due to thermal instability. That is, the pulsed saturation capability for a given pulse duration is a curve with a bend or knee in the I_d , V_{ds} operating space. This was not always the case. Historically, the pulsed saturation capability for a power MOSFET device was simply the calculated safe constant power capability. This was because for early MOSFET planar technologies and in some case first generation trench

technologies, the pulsed saturation capability of such devices measured greater (by sufficient margin) than the calculated safe thermal capability (refer to figure 9) for the devices. Therefore, publishing the safe calculated thermal capability was sufficient for the FBSOA plot. As later generation, much higher gain trench MOSFET technologies were introduced it was found that measured saturation capability fell below the safe calculated thermal capability for devices. Therefore, empirical pulsed saturation data had to be included in the FBSOA plot.

To form a pulsed saturation capability curve on the FBSOA plot the safe calculated thermal capability is determined. Then measured $I_d(\text{fail})$ data is collected and then de-rated. Both sets of data when plotted in the I_d , V_{ds} space, will intersect. It is this intersection of the calculated constant power curve and the de-rated measured $I_d(\text{fail})$ data that forms the curve “knee”. Thus, the “knee” indicated in a pulsed saturation capability curve has no physical meaning (refer to figure 10).

The power MOSFET FBSOA plot has limits to its utilization in real world application analysis. Most obvious is the FBSOA plot, for practical reasons, provides data for only a few pulse durations. A user can at least understand a range of pulsed saturation capability for some device, but if data for a specific pulse duration is required, it must be measured. Note that power MOSFET thermal instability behavior is difficult to physically model and such behavior is not included in device simulation models. Less obvious is that the power MOSFET saturation power function for most real-world applications is not square-wave, yet the FBSOA plot provides data only for a square-wave power function.

Figure 11 shows expected power functions for real-world situations where a power MOSFET is operated in saturation, compared to the standard square-wave power function utilized in device characterization. These include active clamp inductive load switch-off, in-rush current control, and inductive load hard switched transitions (e.g., in some DC/DC power supply applications). Most real-world application saturation operation results in triangular power functions. In general, these functions have greater SOA compared to the square-wave function. Thus, the data sheet FBSOA plot data could be considered as worst-case analysis for most applications. However, application analysis based on data sheet FBSOA plot may result in a conservative device selection. If possible, it is better practice to compare actual device performance in the application circuit and operating conditions to make an optimal MOSFET selection.

Power MOSFET device saturation capability often must be considered in application fault analysis. That is, standard thermal analysis of the fault mode operation may indicate no expected issue with MOSFET device performance, but in practical testing the device fails. This is commonly due to unexpected thermal runaway failure. Consider a short circuit fault, where the MOSFET switch is connected through a low ohmic path either to battery positive or battery

negative (depending on lead configuration) resulting in much greater drain current (and associated power) whilst the device remains activated, and the short fault persists. In modern systems, circuits are designed so that a short circuit fault is recognized, and action taken to switch off the MOSFET switch or switches often occurs within 5–10 μ s, and in some cases less than 3 μ s. Thus, even though instantaneous power may be quite large (perhaps tens of kilowatts), the energy is low (due to short fault duration) and in general failure of the MOSFET due to pure thermal consideration does not occur.

Consider figure 11, which shows oscilloscope traces for a short circuit fault condition (of duration = ~12 μ s) for a second-generation trench technology device. In this application example the MOSFET is configured low side, so the fault is a short to battery. Important to consider in this case is that the gate drive pull down resistance is quite large, at ~400 ohms; this results in the relatively slow switch-off observed in the scope traces. The first observation is the device survives the 12 μ s short circuit pulse at high drain voltage and current, where power peaked at nearly 10 kW. The second observation is that the device does eventually fail, indicated by the rapid increase of drain current off scale and the corresponding rapid decrease of drain voltage (the device shorts out). The further and key observation is that the failure occurs *well* after the device is deactivated, when gate voltage is at or close to zero volts and device power is close to zero. The slow switch-off requires the device to operate in saturation for some time, and before the device can completely shut-off (where $I_d = 0$), the conditions are met such that the device goes into thermal runaway and fails short. In this example, another run was made with the pull-down resistance reduced significantly to 10 ohms. In

this case, for the same short circuit fault, the device survived. This is because the time duration in saturation at switch-off was significantly reduced.

A power MOSFET operates to some degree in saturation in nearly every application function. A power MOSFET may also unexpectedly operate in saturation in response to some system fault event. If the power MOSFET is operating in saturation with V_{gs} voltage < V_{gs} (ZTC) voltage, then depending on other operating conditions the device may suffer thermal runaway and fail. For this reason, it is important to understand pulsed saturation capability characterization and associated limitations to typical published FBSOA data.

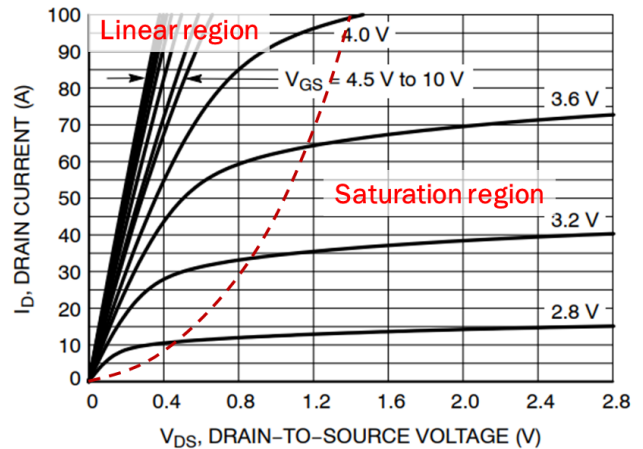


Figure 1. Typical Power MOSFET Forward Biased I_d , V_{ds} Function Showing the Delineation of the Linear and Saturation Operation Regions

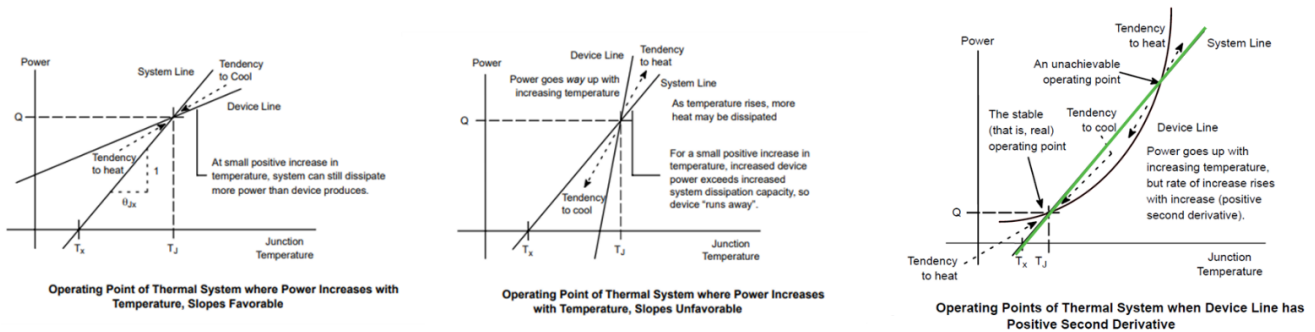


Figure 2. General Representation of Device Power as Function Temperature and System Capability to Sink Power and Relationship to Stable or Unstable (Thermal Instability) Operating Points

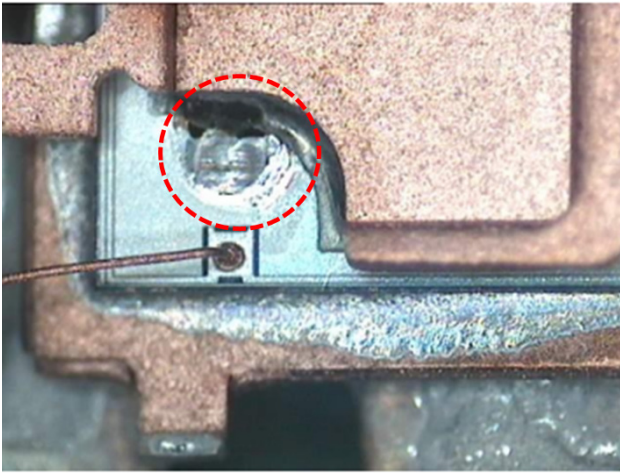


Figure 3. Photograph of a Power MOSFET Device (after De-capsulation) that Failed During Saturation Operation (Thermal Runaway). The Failure Site is Circled in Red.

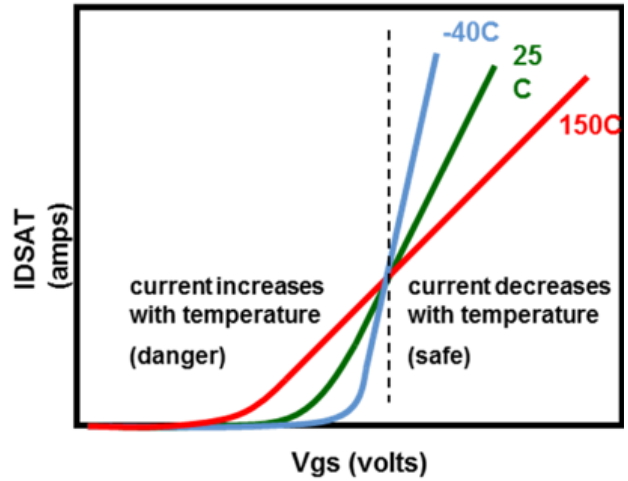


Figure 4. A Generic Representation of Power MOSFET Transconductance Curves at Different Junction Temperatures. The V_{gs} Value Where the Curves Intersect is Known as $V_{gs}(ZTC)$.

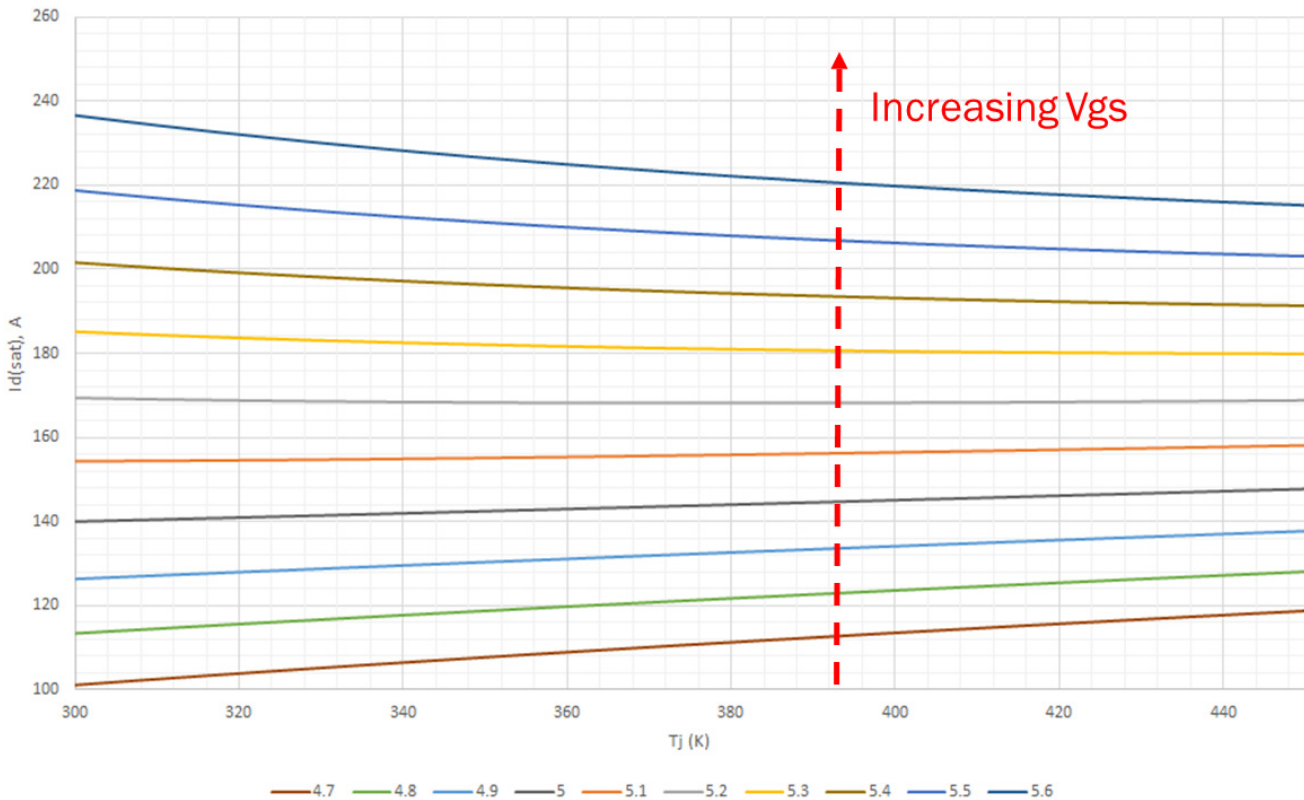


Figure 5. An Example Data Set Showing I_{dsat} as a Function of Temperature for Increasing V_{gs} Bias. This is Another Representation of $V_{gs}(ZTC)$, Which in This Case is at $V_{gs} = \sim 5.2$ V, Where I_{dsat} is Independent of Temperature.

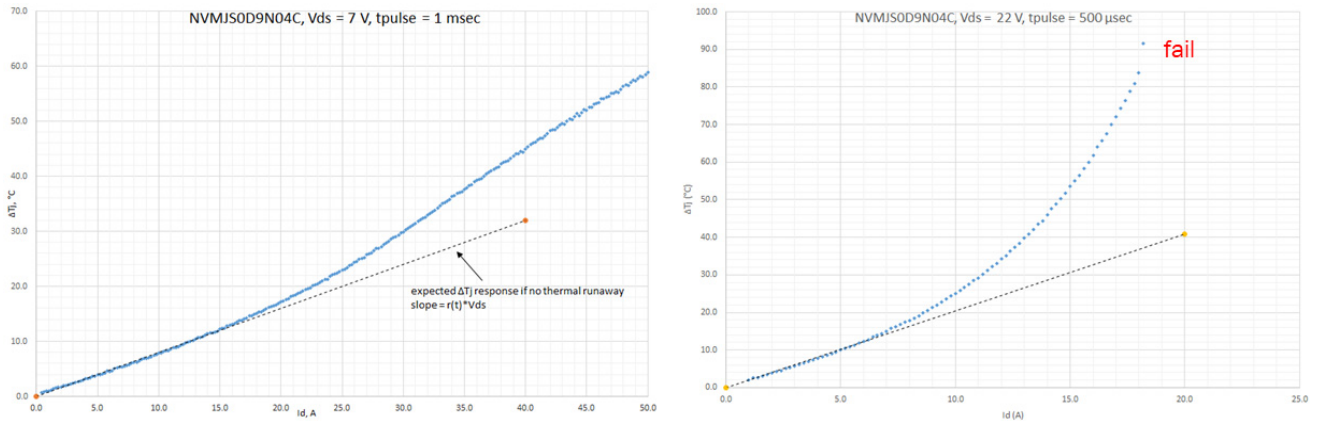


Figure 6. Visualization of Thermal Instability Behavior. Initially Delta Tj Increases Linearly with Applied Power, but as the Device Enters Thermal Instability Operation, Delta Tj Increases More Rapidly Than the Expected Linear Response.

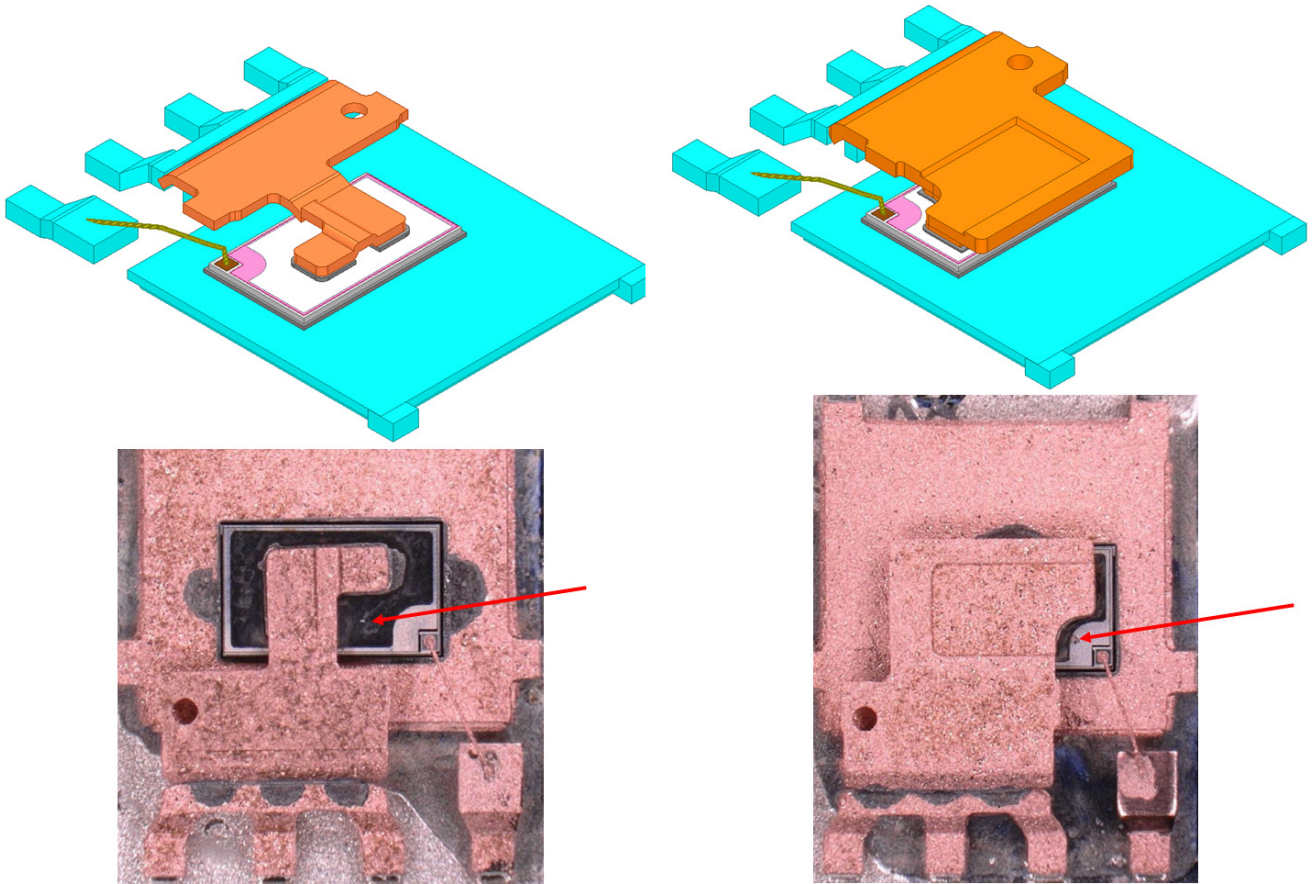


Figure 7. Comparison of Thermal Runaway Failure Site Location (Indicated by Red Arrows) for Two Device Utilizing Same Die and Same Package but Different Source Clip Designs

AND90187/D

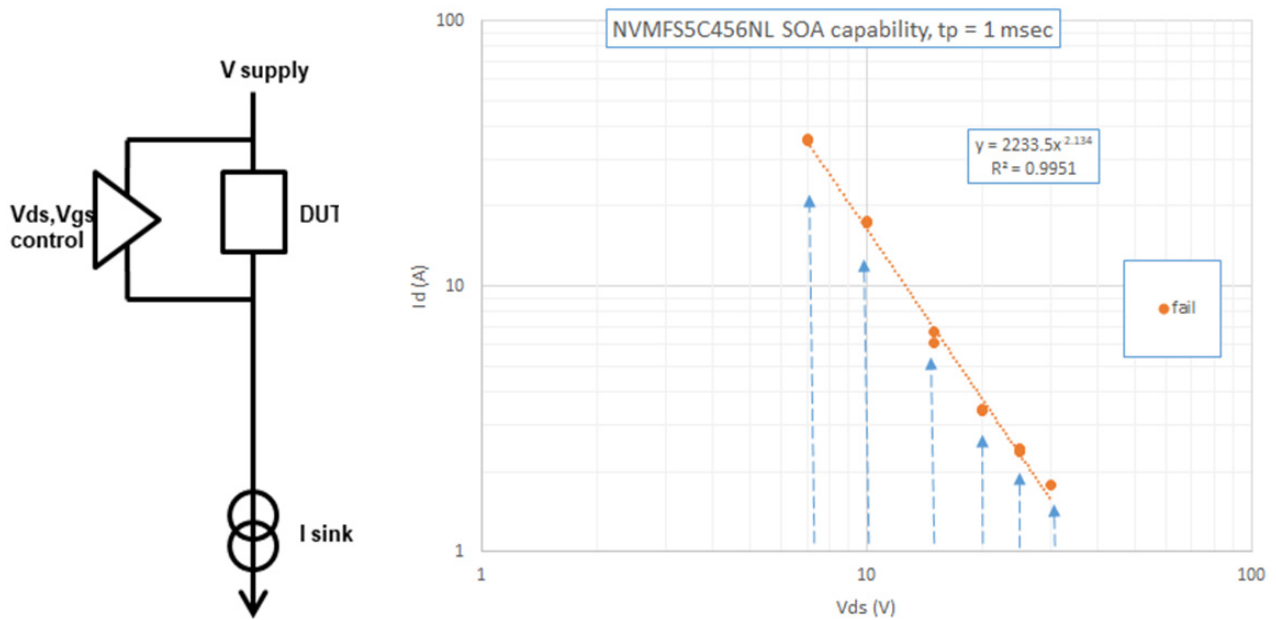


Figure 8. Left Side Shows the General Block Diagram for a Circuit to Evaluate Power MOSFET Pulsed Saturation Operation Capability. The Right Plot Illustrates the Procedure: For a Fixed Pulse Duration, I_d is Incremented to Failure Point for Different V_{ds} Values.

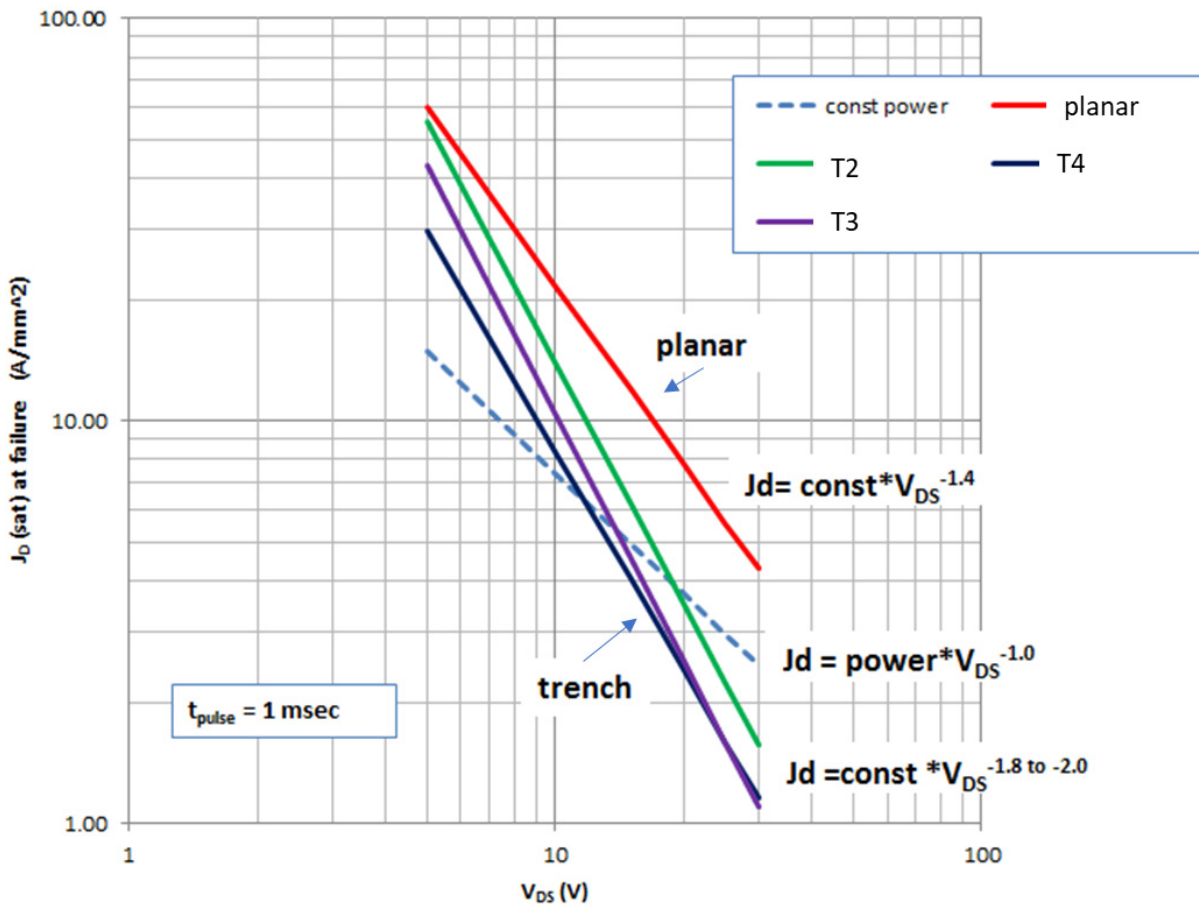


Figure 9. Typical Planar and Trench Technology Pulsed Saturation Capability (at Failure) Compared to Calculated Safe Thermal Capability (Constant Power Given by $dt_j / r(t)$)

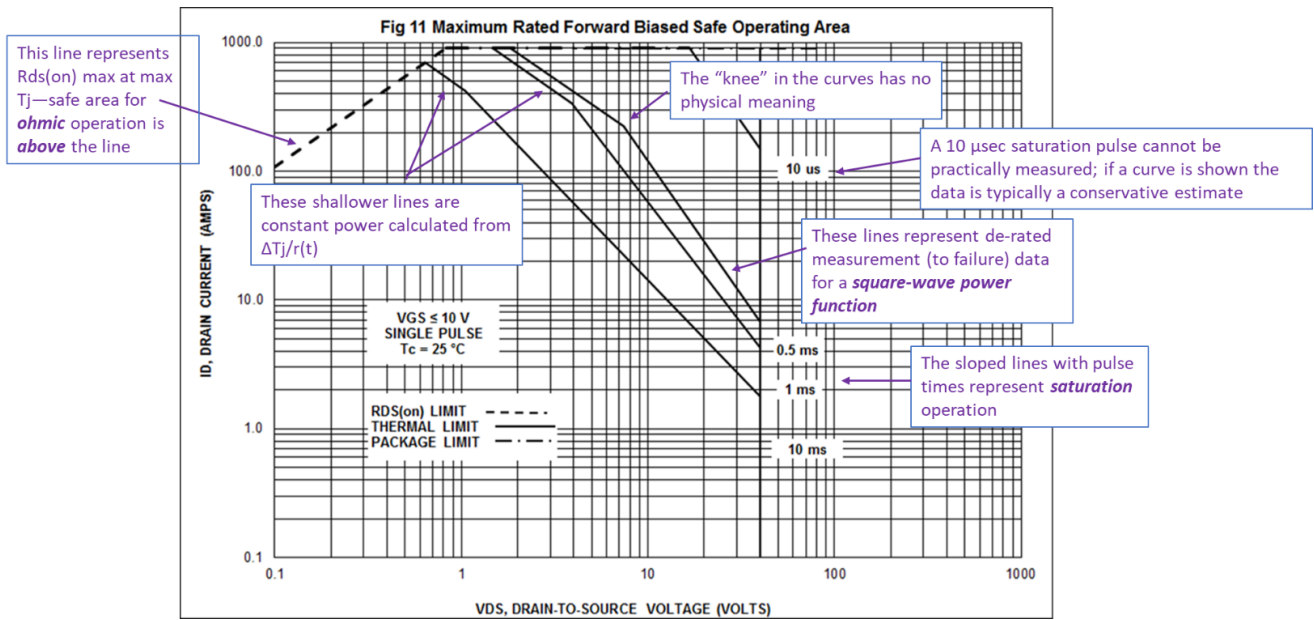


Figure 10. A Typical Power MOSFET FBSOA Plot

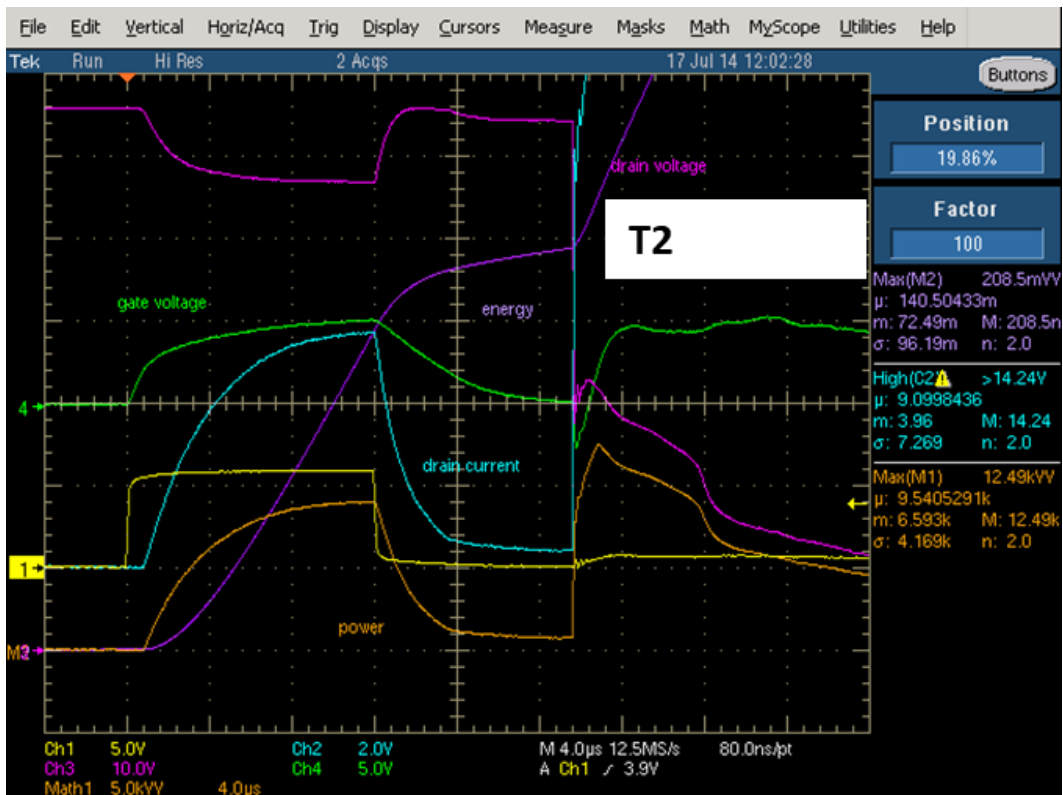


Figure 11. Scope Traces for a Low-side Power MOSFET Subjected to Low Ohmic Short to Battery Positive. Note the Device Fails Well after Gate is Commanded Off in Response to the Fault.

onsemi, **Onsemi**, and other names, marks, and brands are registered and/or common law trademarks of Semiconductor Components Industries, LLC dba "**onsemi**" or its affiliates and/or subsidiaries in the United States and/or other countries. **onsemi** owns the rights to a number of patents, trademarks, copyrights, trade secrets, and other intellectual property. A listing of **onsemi**'s product/patent coverage may be accessed at www.onsemi.com/site/pdf/Patent-Marking.pdf. **onsemi** reserves the right to make changes at any time to any products or information herein, without notice. The information herein is provided "as-is" and **onsemi** makes no warranty, representation or guarantee regarding the accuracy of the information, product features, availability, functionality, or suitability of its products for any particular purpose, nor does **onsemi** assume any liability arising out of the application or use of any product or circuit, and specifically disclaims any and all liability, including without limitation special, consequential or incidental damages. Buyer is responsible for its products and applications using **onsemi** products, including compliance with all laws, regulations and safety requirements or standards, regardless of any support or applications information provided by **onsemi**. "Typical" parameters which may be provided in **onsemi** data sheets and/or specifications can and do vary in different applications and actual performance may vary over time. All operating parameters, including "Typicals" must be validated for each customer application by customer's technical experts. **onsemi** does not convey any license under any of its intellectual property rights nor the rights of others. **onsemi** products are not designed, intended, or authorized for use as a critical component in life support systems or any FDA Class 3 medical devices or medical devices with a same or similar classification in a foreign jurisdiction or any devices intended for implantation in the human body. Should Buyer purchase or use **onsemi** products for any such unintended or unauthorized application, Buyer shall indemnify and hold **onsemi** and its officers, employees, subsidiaries, affiliates, and distributors harmless against all claims, costs, damages, and expenses, and reasonable attorney fees arising out of, directly or indirectly, any claim of personal injury or death associated with such unintended or unauthorized use, even if such claim alleges that **onsemi** was negligent regarding the design or manufacture of the part. **onsemi** is an Equal Opportunity/Affirmative Action Employer. This literature is subject to all applicable copyright laws and is not for resale in any manner.

PUBLICATION ORDERING INFORMATION

LITERATURE FULFILLMENT:
Email Requests to: orderlit@onsemi.com

TECHNICAL SUPPORT
North American Technical Support:
Voice Mail: 1 800-282-9855 Toll Free USA/Canada
Phone: 011 421 33 790 2910

Europe, Middle East and Africa Technical Support:
Phone: 00421 33 790 2910
For additional information, please contact your local Sales Representative

onsemi Website: www.onsemi.com